Gallium-modified zeolites for the selective conversion of bio-based dihydroxyacetone into C_1-C_4 alkyl lactates

Author(s):
Dapsens, Pierre Y.; Kusema, Bright T.; Mondelli, Cecilia; Pérez-Ramírez, Javier

Publication date:
2014-07

Permanent link:
https://doi.org/10.3929/ethz-a-010788767

Originally published in:
Journal of Molecular Catalysis. A, Chemical 388-389, https://doi.org/10.1016/j.molcata.2013.09.032

Funding acknowledgement:
140496 - Biomass to chemicals over tailored hierarchical zeolite-based catalysts (SNF)

Gallium-modified zeolites for the selective conversion of bio-based dihydroxyacetone into C_1-C_4 alkyl lactates

Pierre Y. Dapsens, Bright T. Kusema, Cecilia Mondelli*, Javier Pérez-Ramírez*

ETH Zurich, Institute for Chemical and Bioengineering, Department of Chemistry and Applied Biosciences, Wolfgang-Pauli-Strasse 10, CH-8093 Zurich, Switzerland

* Corresponding authors. E-mails: cecilia.mondelli@chem.ethz.ch, jpr@chem.ethz.ch

Abstract

Recently, we have demonstrated that post-synthetic alkaline-assisted galliation of FAU-type zeolites generates outstanding Lewis-acid tin-free catalysts for the production of ethyl lactate from dihydroxyacetone under mild conditions. Herein, we show that this preparation method is superior with respect to conventionally practiced strategies for metal incorporation in zeolites, such as dry impregnation and ion exchange with gallium salts. By means of IR spectroscopy of adsorbed pyridine and ^{71}Ga MAS NMR, it is evidenced that, although gallium migration to the zeolite framework likely occurs also during the traditional preparation, the highly selective tetra-coordinated gallium centers identified for the galliated zeolite in alkaline medium are less abundant in the impregnated and exchanged samples. Furthermore, alkaline-assisted galliation was successfully applied to other zeolite frameworks including MFI, MOR, FER, and BEA, thus evidencing the versatility of the approach. The GaUSY catalyst also proved to be the best tin-free system for the production of *n*-propyl and *n*-butyl lactates. In addition, its remarkable performance in ethanol remained unaltered even upon a fivefold increase of the DHA feed concentration, *i.e.* from the typically applied 3 wt.% to 15 wt.%, thus strengthening its potential for an industrial application.

Keywords: Isomerization; Alkyl lactates; Hierarchical zeolites; Gallium; Lewis acidity.

1. Introduction

The production of chemicals and materials from lignocellulosic biomass attracts substantial interest [1-6]. Lactic acid has been identified as one of the most relevant platform molecules resulting from bio-based feedstocks leading to a variety of known chemicals as well as novel bio-polymers [7]. Among these derivatives, short-chain alkyl lactates (ALs) represent promising green solvents, owing to their strong ability to dissolve compounds of diverse chemical characteristics, *e.g.* cellulose acetate, nitrocellulose, oils, dyes, gums, and paints [7,8]. Ethyl lactate (EL), in particular, shows a real potential to widely replace the toxic and halogenated organic media currently used in industry [9]. Besides for their solvating properties, methyl lactate (ML) can be dehydrated to methyl acrylate, a precursor in the manufacture of acrylate fibers, while propyl and butyl lactates (PL and BL) also find broad uses as flavoring agents and in the fine chemical industry. Optically active PL is especially employed as a chiral intermediate in the synthesis of drugs and pesticides [8].

At present, the industrial production of ALs comprises the microbial fermentation of glucose or sucrose to lactic acid, followed by H_2SO_4-catalyzed esterification. This enzymatic route is capital intensive and environmentally unattractive due to the various separation, neutralization, and purification steps imposed by the use of a highly corrosive acid and by the production of large amounts of gypsum waste [7-9]. Therefore, many researchers have been focusing on the development of more sustainable routes to ALs based on chemo-catalysis. The acid catalyzed isomerization of the C_3 sugar-derived compounds dihydroxyacetone (DHA) and glyceraldehyde (GLY) in alcoholic media represents the most promising alternative [10,11]. Both the triose substrates can be obtained from C_6 sugars (*i.e*. fructose and glucose) via retro-aldolization but their most appealing source is glycerol, which is readily available as a by-product of the manufacturing of bio-fuels [12,13]. The reaction proceeds via the Brønsted- or Lewis-acid catalyzed dehydration of DHA or GLY into pyruvic aldehyde (PAL) (Scheme 1). Noteworthy, it has been demonstrated that, due to the higher

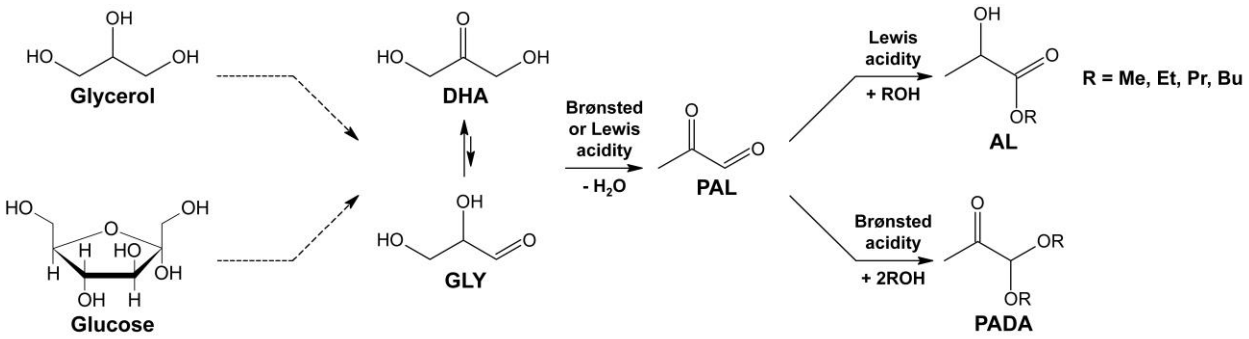

Scheme 1 Reaction network for the catalytic conversion of bio-derived C_3 substrates into alkyl lactates.

thermodynamic stability of DHA, GLY actually undergoes rapid isomerization into this isomer prior to the dehydration step [14]. The AL product forms upon nucleophilic attack of the alcohol on the aldehydic carbon of PAL followed by 1-2 hydride shift over Lewis-acid sites [10-12,15]. The presence of strong Brønsted-acid centers favors the addition of two alcohol molecules to PAL leading to the by-product pyruvic acid dialkyl acetal (PADA). In view of the greatly higher cost of GLY compared to DHA and owing to the similar AL yields attained from either of the starting materials, DHA constitutes the typically preferred substrate [11,16-18].

Homogeneous metal halide catalysts (*e.g.* $SnCl_2$, $SnCl_4 \cdot 5H_2O$) have been firstly investigated for this reaction, which achieved yields of alkyl lactates up to 91% at 363 K in a few hours [10]. Based on these findings, efficient heterogeneous tin-based catalysts were successfully developed by embedding of this metal into the structure of porous materials. Purely Lewis-acidic solids as Sn-beta and Sn-MCM-41 have been reported to enable the full conversion of DHA in ethanol with almost complete selectivity to EL under mild reaction conditions (363 K, 4-6 h) [19,20]. However, since the industrial application of Sn-based materials might be hampered by the scarcity of tin, commercial aluminosilicate zeolites have also been evaluated for the production of ALs [15,16]. Zeolites possessing large amounts of extra-framework aluminum and, thus, enhanced Lewis acidity have been

found promising. In particular, Pescarmona *et al.* have identified CBV600 as the best catalyst among various USY zeolites, displaying yields of 82, 81, 83, and 71% for ML, EL, PL, and BL, respectively, at 383 K. A higher ML yield (96%) was observed by West *et al.* over CBV712 at a slightly higher temperature (393 K) [15,16]. Some of us have recently demonstrated the benefits of post-synthetic modification of commercial zeolites to generate even superior Lewis-acidic tin-free catalysts for the isomerization of DHA in water and ethanol. We have shown that alkaline-treatment of MFI-type zeolites creates unique aluminum sites leading to lactic acid selectivities exceeding 90%, comparable to Sn-based zeolites [21]. For EL production, alkaline-assisted galliation can be conveniently used to introduce highly selective sites in FAU-type zeolites. This procedure generates tetra-coordinated Lewis-acid gallium centers linked to the framework, which reach the state-of-the-art EL selectivity of 82% at only 358 K when using CBV720 (H-USY, Si/Al = 17) as the starting zeolite and are stable in repeated catalytic runs [22].

Herein, we show that the high selectivity of GaUSY zeolites obtained by alkaline-assisted galliation in the conversion of DHA into EL cannot be matched by applying other more conventional post-synthetic modification methods such as impregnation or ion exchange with gallium sources. The differences in catalytic performance are rationalized through in-depth characterization studies. The versatility of alkaline-assisted galliation is extrapolated to other zeolite frameworks, *i.e.* MFI, FER, BEA, and MOR. Application of GaUSY for DHA isomerization in other short-chain alcohols leads to a comparable ML yield and up to 20% higher PL and BL yields with respect to the best commercial zeolite (CBV600) at reduced temperature (363 K). Experiments with concentrated DHA feed render identical performance.

2. Experimental

2.1. Catalysts

MFI (CBV3024E, Si/Al = 17, NH_3-form), FAU (CBV720, Si/Al = 17, H-form), MOR (CBV21A, Si/Al = 10, NH_3-form), and FER (CP914C, Si/Al = 28, NH_3-form) were purchased from Zeolyst International, whereas BEA (HSZ940, Si/Al = 21, H-form) was supplied by Tosoh. These zeolites, referred to as parent (code P), were used as received for post-synthetic modification which comprised alkaline-assisted metallation, dry impregnation, or ion exchange. The first was performed in aqueous NaOH solutions (0.1-0.6 M, 30 cm^3 per gram of dried zeolite) containing 0.04 M of $Ga(NO_3)_3$ or $Al(NO_3)_3$ (Sigma, 99.9%) at 338 K for 30 min in an Easymax 102 reactor from Mettler Toledo. The resulting materials were then converted into their protonic form by three consecutive treatments in an aqueous solution of NH_4NO_3 (0.1 M, 298 K, 6 h, 100 cm^3 per gram of zeolite) and subsequent thermal treatment in static air at 823 K during 5 h (5 K min^{-1}). These modified samples are denoted by the code AT*x* (where *x* represents the first digit after the comma of the NaOH concentration), extended by Ga or Al.

FAU-DI and FAU-IE were respectively prepared by dry impregnation of $Ga(NO_3)_3$ (6 wt.% Ga) and ion exchange (0.1 M aqueous $Ga(NO_3)_3$, 298 K, 6 h, 100 cm^3 per gram of zeolite, 3 times) of FAU, followed by drying at 338 K overnight and subsequent calcination as described above.

Gallium trioxide (Strem Chemicals, 99.998%) and FAU (Zeolyst, CBV600, Si/Al = 2.6, H-form) were used as received as reference catalysts.

2.2. Characterization

The content of Si, Al, and Ga in the samples was determined by inductively coupled plasma optical emission spectroscopy (ICP-OES) using a Horiba Ultra 2 instrument equipped with a photomultiplier tube detector. Nitrogen isotherms at 77 K were measured using a Quantachrome Quadrasorb-SI gas adsorption analyzer. Prior to the measurements, samples were degassed in vacuum

(10^{-1} mbar) at 573 K for 3 h. Powder X-ray diffraction (PXRD) was measured using a PANalytical X'Pert PRO-MPD diffractometer with Ni-filtered Cu Kα radiation (λ = 0.1541 nm). Data was recorded in the 5-70° 2θ range with an angular step size of 0.05° and a counting time of 7 s per step. Fourier transform infrared (FTIR) spectroscopy measurements of adsorbed pyridine were carried out using a Bruker IFS66 spectrometer equipped with a liquid N_2-cooled mercury cadmium telluride (MCT) detector. Self-supporting zeolite wafers (20 mg, 5 ton cm^{-2}, 1 cm^2) were pretreated at 10^{-3} mbar and 693 K for 4 h. After cooling down to room temperature, the sample was saturated with pyridine vapor and then evacuated at room temperature for 15 min and subsequently at 473 K for 30 min. Spectra were recorded in the 650-4000 cm^{-1} range (4 cm^{-1} resolution) by co-addition of 32 scans. High-resolution magic angle spinning ^{71}Ga nuclear magnetic resonance (MAS NMR) spectroscopy was measured using a Bruker AVANCE 700 NMR spectrometer equipped with a 4-mm probe head and 4-mm ZrO_2 rotors at 213.5 MHz. Spectra were acquired using a spinning speed of 10 kHz, 20000 accumulations, 1 µs pulses, a recycle delay of 0.02 s, and $Ga(NO_3)_3 \cdot H_2O$ as a reference. Transmission electron microscopy (TEM) was undertaken using a FEI Tecnai F30 microscope operated at 300 kV (field emission gun). The samples were prepared by depositing a few droplets of zeolite suspension in methanol on a carbon-coated copper grid, followed by evaporation at room temperature.

2.3. Catalytic testing

Catalytic tests were performed under autogenous pressure in 15-cm^3 thick-walled glass vials (Ace, pressure tubes, front seal) dipped in an oil bath heated at the desired reaction temperature (363, 378, or 393 K). The vials were loaded with 120 mg of dihydroxyacetone (DHA, Sigma-Aldrich, 97%, dimer), 80 mg of catalyst, and 3.88 g of solvent. The latter comprised methanol, ethanol (both purchased from Scharlau, 99.9%), propan-1-ol, (ABCR, 99.9%), or butan-1-ol (Merck, 99.5%). The mixture was allowed to react under vigorous magnetic stirring during 24 h. After that time, the

reaction was quenched using an ice bath and the catalyst removed by means of a Chromafil Xtra 0.25 μm syringe filter. The unconverted DHA and pyruvaldehyde (PAL) were isolated by high-performance liquid chromatography (HPLC) in a Merck LaChrom system equipped with a Biorad Aminex HPX-87H column heated at 308 K, using an aqueous eluent of 0.005 M H_2SO_4 (pH 2) flowing at 0.6 cm^3 min^{-1}. Quantification was obtained by integration of their UV-Vis absorbance band at 272 nm using butan-2-one (Merck, 99.5%) as an internal standard. The produced pyruvic aldehyde diethyl acetal (PADA) and alkyl lactate (AL) were analyzed using a gas chromatograph (GC, HP 6890) equipped with an HP-5 capillary column and a flame ionization detector. Methyl lactate (ML, Sigma-Aldrich, 97%), ethyl lactate (EL, TCI, 97%), *n*-propyl lactate (PL, TCI, 95%), and *n*-butyl lactate (BL, Sigma-Aldrich, 98%) were employed as references. He was used as the carrier gas (flow rate = 4.3 cm^3 min^{-1}, pressure = 1.4 bar) and an injection volume of 0.3 μL was applied. The initial temperature of 328 K was held for 2 min before heating to 473 K (30 K min^{-1}). While the yields of ML and EL were determined using *iso*-octane (Fluka, 99.5%) as an internal standard, those of PL and BL were assessed using diethyl malonate (Sigma-Aldrich, 99%) and butan-2-one as internal standards, respectively. The yield of PADA was determined utilizing the response factor calculated for pyruvic aldehyde dimethyl acetal, since PADA was not commercially available. The conversion of DHA was calculated as the mole of DHA reacted divided by the mole of DHA fed, while the yield of AL (PADA) as the moles AL (PADA) formed divided by the initial mole of DHA. 1,1,2,2-tetraalkoxypropane was identified as the only other by-product by GC-MS (GC, HP 6890, MS, HP 5973).

3. Results and discussion

3.1. Production of EL over Ga-modified FAU zeolites

Recently, we have applied post-synthetic alkaline treatments to tune the acid properties of the FAU zeolite CBV720 (Si/Al = 17, denoted as FAU-P) to attain improved performances for the DHA isomerization in ethanol [22]. As simple base leaching led to an excessive collapse of the zeolite structure, the utilization of pore directing agents (PDA) as a means to preserve the structural integrity of the framework was envisaged and PDAs were selected that could give rise to Lewis acidity upon their incorporation. Both Al^{3+} and Ga^{3+} cations enabled the development of further mesoporosity, while substantially retaining the zeolite crystalline structure (FAU-AT2Al and FAU-AT2Ga respectively, Table 1, entries 2-3). Furthermore, they were introduced into the framework to significant extent. Still, more metal cations were incorporated into FAU upon galliation, which corresponded to a greater increase in the amount of Lewis-acid sites for FAU-AT2Ga compared to FAU-AT2Al (135 *versus* 91 μmol g^{-1}, respectively). Accordingly, galliation proved superior in enhancing the performance of the parent zeolite in the transformation of DHA into ethyl lactate at 363 K. Maintaining full conversion, the EL selectivity increased from 27 to 82%, while it was only 59% in the case of FAU-AT2Al (Fig. 1). The highly selective Lewis-acid gallium centers were uncovered to comprise tetra-coordinated species linked to the FAU framework.

In order to investigate the influence of properties of FAU-AT2Ga compared to FAU-P on the selectivity patterns in the production of EL, the concentrations of DHA, PAL, EL, and PADA were monitored over time at 363 K for the two materials (Fig. 2). Besides for these compounds, 1,1,2,2-tetraethoxypropane (TEP) was also observed as by-product originating from the further alkylation of PADA with the alcohol. With respect to the reaction pathway described in the literature [15, 18] and represented in Scheme 1, FAU-P displayed a clear dominance of the side route leading from PAL and TEP to PADA (Fig. 2a), which continued increasing up to a yield of 62% at 24 h, *i.e.* the time

Table 1. Characterization data of the catalysts.

Entry	Catalyst[a]	Si/Al[b] (mol mol^{-1})	Ga content[b] (wt.%)	Crystallinity[c] (%)	S_{meso}[d] (m^2 g^{-1})	V_{micro}[d] (cm^3 g^{-1})
1	FAU-P	17	-	100	128	0.29
2	FAU-AT2Al	8	-	51	161	0.26
3	FAU-AT2Ga	15	6.0	88	137	0.24
4	FAU-DI	14	3.7	100	113	0.27
5	FAU-IE	25	4.0	100	110	0.27
6	Ga_2O_3	-	-	-	20	0
7	MFI-P	15	-	100	75	0.18
8	MFI-AT6	11	-	75	125	0.17
9	MFI-AT6Ga	12	0.35	64	110	0.17
10	MOR-P	10	-	100	42	0.20
11	MOR-AT5Ga	8	0.24	94	64	0.18
12	FER-P	28	-	100	34	0.13
13	FER-AT5Ga	27	0.13	100	33	0.13
14	BEA-P	21	-	100	57	0.22
15	BEA-AT1Ga	10	3.49	86	67	0.21

[a] P = parent, AT1-6 = alkaline treatment with 0.1-0.6 M NaOH, Al/Ga = NaOH treatment in the presence of 0.04 M $Al(NO_3)_3$/$Ga(NO_3)_3$, DI = dry impregnation with $Ga(NO_3)_3$, IE = ion exchange with 0.1 M $Ga(NO_3)_3$. [b] Determined by ICP-OES. [c] Relative crystallinity to the parent zeolite derived from XRD. [d] Determined by the *t*-plot method.

required for achieving full DHA conversion. Although the formation of PADA from the intermediate PAL is indicated as reversible [15,18,23], only in the presence of sufficient Lewis acidity preferential conversion of PAL into EL can occur. This is not the case for FAU-P, where the amount of Brønsted-acid sites greatly surpasses that of Lewis-acid centers (216 *versus* 53 μmol g^{-1}). The kinetic profile obtained for FAU-AT2Ga was dramatically different. EL production was largely dominant and the initial rate of formation of this product was more than 7-fold higher

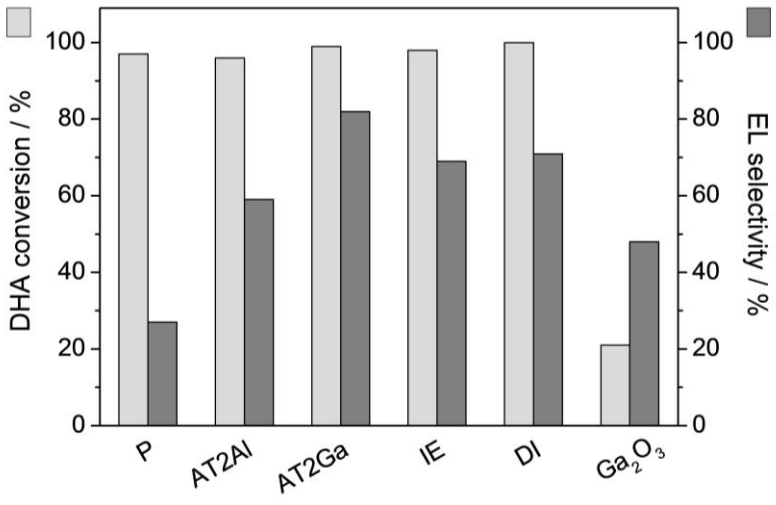

Fig. 1. DHA conversion and EL selectivity over FAU in parent form and after gallium or aluminum incorporation and over gallium oxide.

compared to FAU-P (Fig. 2b) and full conversion of DHA was achieved within 6 h. While moderate amounts of PAL and TEP were formed at early stages of the reaction, the yield of those intermediates rapidly decreased at the expense of that of PADA, which attained a maximum value of 18% at 6 h. Thereafter, the PADA yield was progressively depleted, while the EL yield increased concomitantly, thus supporting the reversible nature of the reaction from the dialkyacetal to pyruvic aldehyde. Interestingly, an identical product distribution was achieved at 24 h over the galliated catalyst when using GLY as the substrate, confirming the reported suitability of this alternative triose for ethyl lactate production.

Although alkaline-assisted galliation is a scalable treatment and no major aspect of this method seems to hinder the production of galliated FAU zeolites at practical costs [24], we evaluated whether other post-synthetic methods commonly practiced at technical scale could produce Ga-modified materials displaying similar activity and selectivity. Thus, two catalysts were prepared by dry impregnation (FAU-DI) and ion exchange (FAU-IE) of the FAU zeolite with gallium nitrate. TEM

analysis (Fig. 3) evidenced no major alterations of the crystalline structure for FAU-IE compared to the parent material and the presence of gallium oxide nanoparticles of 5-10 nm size at the surface of the zeolite crystals for FAU-DI. Both impregnated and ion-exchanged samples contained similar gallium contents (Table 1, entries 4-5), which were only moderately inferior compared to FAU-AT2Ga. Interestingly, as the amount of gallium incorporated in FAU-IE is larger than that expected to arise from the exchange process (in which one Ga^{3+} cation should replace three H^{+} cations) and no distinct gallium phases were identified over this sample, it is speculated that significant migration of

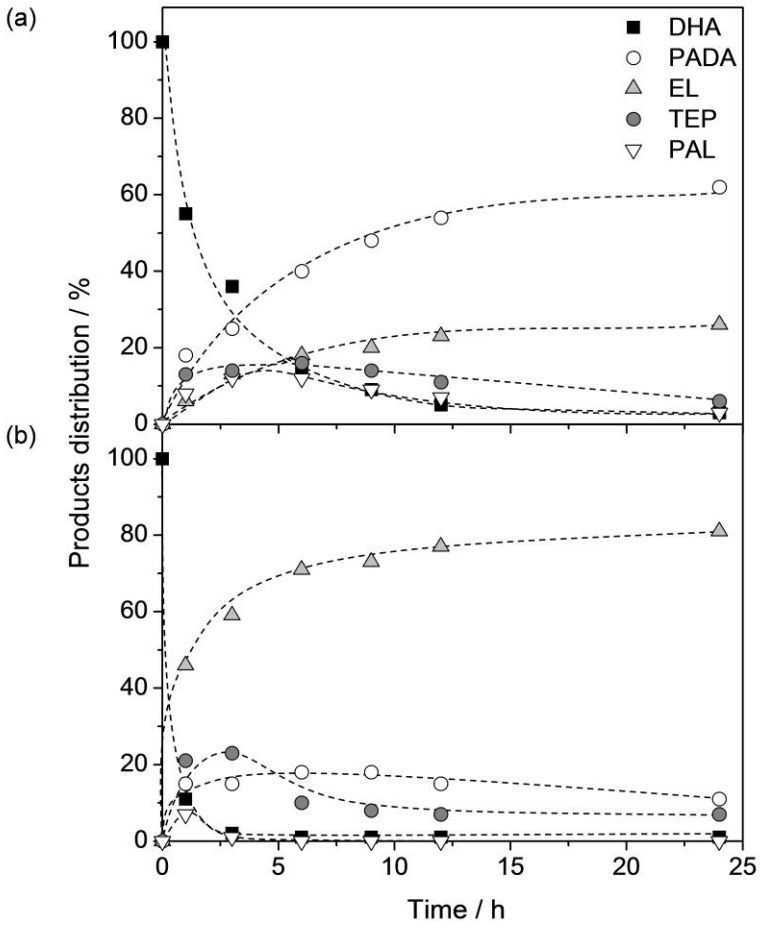

Fig. 2. Concentration profiles of reactant and products during the conversion of DHA in ethanol over (a) FAU-P and (b) FAU-AT2Ga.

gallium atoms into framework defects of the zeolite occurred [25]. Upon catalytic evaluation in the isomerization of DHA in ethanol, FAU-IE and FAU-DI attained similar EL selectivities of 69% and 71%, respectively, at almost full DHA conversion (Fig. 1). The performance of these materials, even though inferior to FAU-AT2Ga, was quite remarkable. The high selectivity of FAU-IE seems to support gallium incorporation into the zeolite framework giving rise to Lewis-acid centers. The catalytic results for FAU-DI were quite surprising, considering the low DHA conversion (21%) and EL selectivity (47%) reached over bulk gallium oxide (Fig. 1). Still, the impregnated Ga_2O_3 phase is likely to feature low crystallinity and high defectivity and may thus contain a variety of Lewis- and

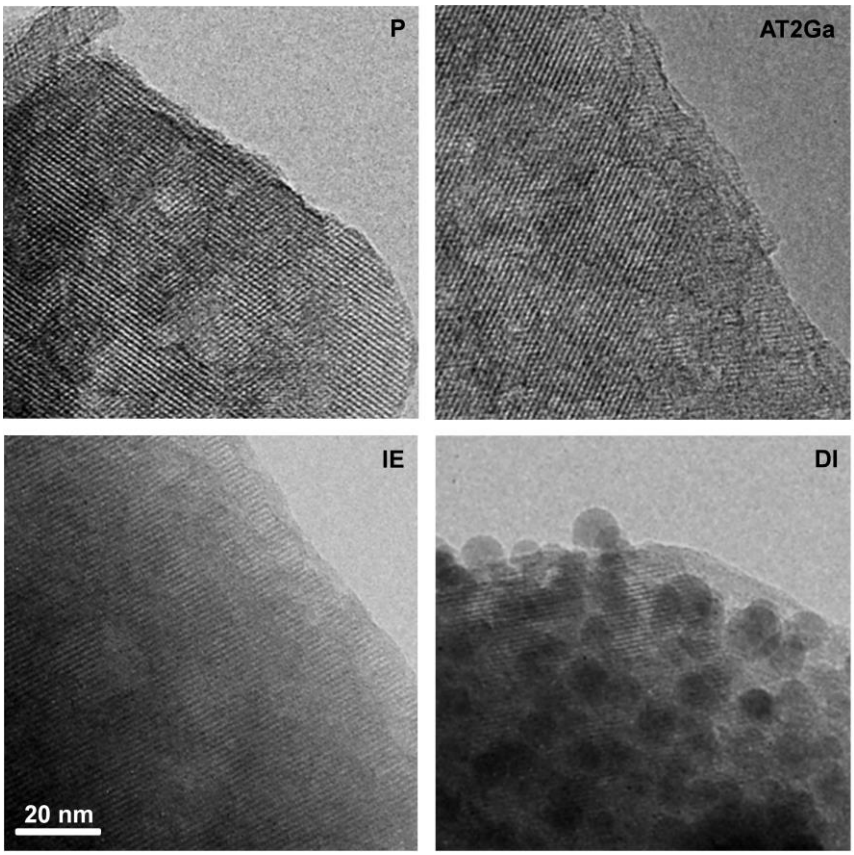

Fig. 3. TEM micrographs of FAU in parent form and after gallium incorporation by different methods. The scale bar applies to all of the micrographs.

Brønsted-acid sites [19,26]. Thus, in-depth characterization of the acidity of the catalyst was performed to establish properties-function relationships.

The catalysts were investigated by FTIR spectroscopy of adsorbed pyridine to quantify the type and amount of acid sites (Fig. 4b). Based on the concentration of Lewis-acid centers derived from the absorption at 1456 cm^{-1}, the following order was obtained: FAU-P (53 µmol g^{-1}) < FAU-IE (83 µmol g^{-1}) < FAU-DI (107 µmol g^{-1}) < FAU-AT2Ga (135 µmol g^{-1}). While the amount of Lewis-acid sites was shown to linearly correlate with the EL selectivity for samples prepared by alkaline-assisted galliation in the presence of variable concentrations of the trivalent cation [21], the agreement of this trend with the EL yields is more qualitative. A positive contribution to the selectivity of the process from the reduced content in Brønsted-acid sites in FAU-DI and FAU-IE compared to FAU-P (143, 180, and 216 µmol g^{-1}, respectively, based on the absorption at 1458 cm^{-1}) should be minimal, as FAU-AT2Ga featured unmodified Brønsted-acid properties with respect to the parent sample and still attained very high selectivities. It seems more likely that the nature of the Lewis-acid sites generated by the conventional post-synthetic methods differs to some extent. ^{71}Ga MAS NMR spectroscopy studies demonstrated that the structure of the highly selective Lewis-acid centers in the zeolites prepared by alkaline-assisted galliation is tetrahedral, as mentioned above, and that these sites constitute 83% of the total Lewis-acid sites, the rest being octahedral [22]. Application of this characterization technique to the impregnated and ion-exchanged catalysts led to similar spectra, although only that of FAU-DI had sufficient quality to enable a reliable evaluation (Fig. 4c). Again, two main peaks centered at 175 and -2.5 ppm, respectively associated to tetrahedral (Td) and octahedral (Oh) gallium [27,28], were identified. Nevertheless, the fraction of Ga-Td was calculated to correspond to only 68%. Thus, the conventional methods used for gallium incorporation appear less efficient in creating Lewis-acid sites of optimal nature. The prime role of the latter sites in determining the selectivity of the process is further supported by the fact that the concentration

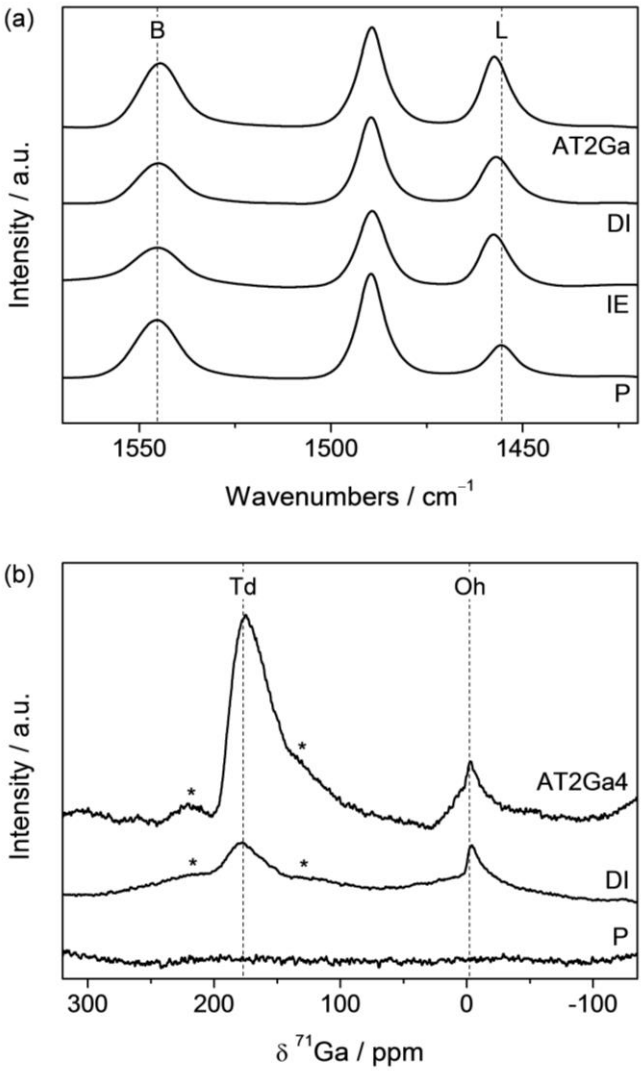

Fig. 4. (a) FT-IR spectra and (b) ^{71}Ga MAS NMR spectra of FAU in parent form and after gallium incorporation by different methods.

profiles of DHA, EL, and PADA over the 24-h reaction for FAU-DI and FAU-IE possessed very similar shape to those of FAU-AT2Ga, only leveling off at different final concentrations (not shown).

3.2. Alkaline-assisted galliation of other zeolite frameworks

We further explored whether alkaline-assisted galliation is applicable to other zeolites frameworks such as FER, BEA, MOR, and MFI. In the treatments, the concentration of Ga^{3+} cations was fixed at the optimal value found for the FAU zeolite (0.04 M), while the strength of the alkaline solution was varied depending on the zeolite structure. It is in fact known that high alkalinities (0.5-0.6 M) are required to induce significant desilication of FER, MFI, and MOR, whereas the high sensitivity of BEA imposes low base concentrations (0.1 M) to prevent amorphization [29,30]. The textural, structural, and compositional properties of the parent and treated zeolites are reported in Table 1, entries 7-15. A moderate increase in mesoporous surface was observed for all of the galliated samples with the exception of FER-AT5Ga (Fig. SI1). The micropore volume was preserved in all cases, in line with the substantial retention of the crystallinity (Fig. SI2). Relatively small amounts of gallium were incorporated into MFI, MOR, and especially FER with respect to FAU-AT2Ga, while BEA-AT1Ga contained a comparable quantity to the latter. In spite of the high base concentration, the dissolution of the more stable zeolites was likely inhibited by the presence of the pore directing agent Ga^{3+}, resulting in a lower gallium incorporation. The zeolites were evaluated in the isomerization of

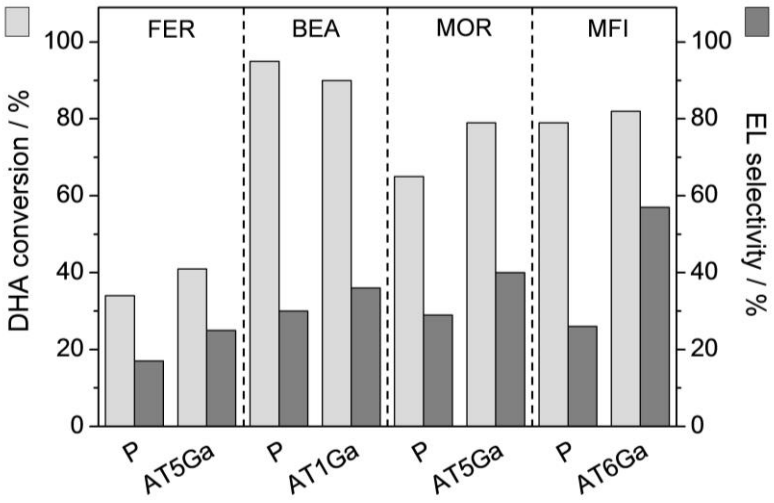

Fig. 5. DHA conversion and EL selectivity over different zeolite frameworks in parent form and after alkaline-assisted galliation.

DHA in ethanol (Fig. 5). Among the parent materials, BEA reached a similar DHA conversion (95%), to FAU-P, while lower values of 79, 65, and 34% were observed for MFI, MOR, and FER respectively. The EL selectivities were in the range of 17-30%, comparable to FAU-P and in line with the low amount of EFAl present in the commercial samples. Generally, enhanced DHA conversion and EL selectivity were observed for the galliated samples, but the levels of modified FAU were not matched. The best EL selectivity was 57% and obtained over MFI-AT6Ga. It is worth mentioning that simple base leaching of MFI in the presence of 0.6 M NaOH (MFI-AT6, Table 1, entry 8) did not lead to improved performances as observed in the water-based isomerization of DHA [21], highlighting the crucial role of the introduced gallium centers for the selectivity of the process in ethanol. Furthermore, as the rather high amount of gallium in BEA-AT1Ga did not translate in proportionally greater selectivities, the framework topology seems to be critical in determining the nature of gallium species and, thus, their catalytic properties.

3.3. Extrapolation to other short-chain alkyl lactates

Based on its unrivalled performance in ethanol, FAU-AT2Ga was evaluated for the production of other relevant short-chain alkyl lactates. The isomerization of DHA was carried out in methanol, *n*-propanol, and *n*-butanol. The parent FAU zeolite was tested for comparative purposes (Fig. 6). Consistent with the data in ethanol, the DHA conversion over FAU-P ranged from 88% to 96% in the different media and the AL selectivities were relatively low (32, 19, and 23% for ML, PL, and BL respectively). As previously observed for the production of EL, the relatively high concentration of Brønsted- *versus* Lewis-acid sites in the parent material favored the conversion of the PAL intermediate into the corresponding pyruvic aldehyde dialkyl acetal and tetraalkoxy propane, which were found to be present in large excess compared to the desired AL product. Upon galliation, a slight increase in DHA conversion was observed in all of the solvents and, more relevantly, the

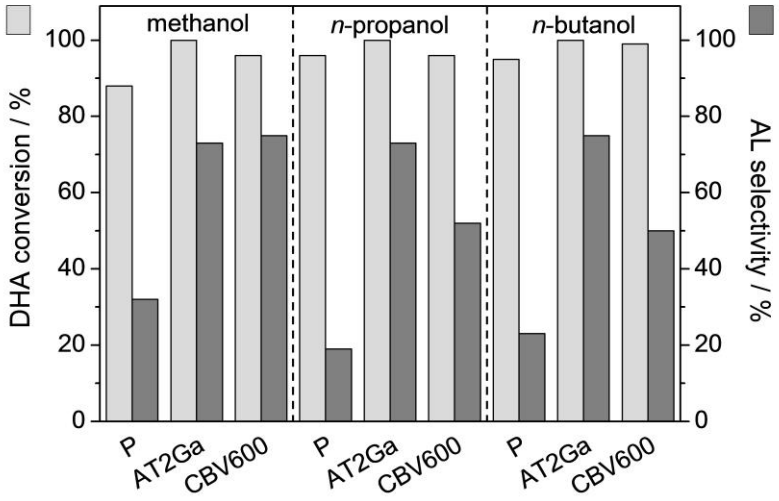

Fig. 6. DHA conversion and AL selectivity over FAU-AT2Ga and CVB600 in C_1-C_4 alcohols.

selectivities were boosted reaching *ca.* 75% for the three ALs, as the formation of PADA and TAP by-products was hindered, as expected.

In order to put these results in perspective with respect to the reference tin-free catalyst, CBV600 was evaluated under the same reaction conditions (Fig. 6). Interestingly, at comparable DHA conversions, the commercial zeolite attained similar ML selectivity (75%) and significantly lower PL and BL selectivities (55% and 50%, respectively). The superiority of FAU-AT2Ga over CBV600 is thus extended from the production of EL to that of PL and BL [22], broadening the scope of application of the highly selective Lewis-acid gallium centers generated by alkaline-assisted metallation.

3.4. Kinetic insights

As the AL is the thermodynamically controlled product and the formation of PADA from PAL is less favorable at high temperature, the AL selectivity can be improved carrying out the reaction at higher temperatures [15]. As shown by Pescarmona *et al.* [15], the EL yield over CVB600 was indeed

proved to progressively increase from 59% to 91% raising the temperature from 363 to 393 K. Accordingly, we evaluated the influence of the reaction temperature on the selectivity to ALs over FAU-AT2Ga. The ML, PL, and BL selectivities steadily increased between 363 and 393 K, while the EL selectivity reached a plateau value of 91% at 378 K (Table 2). With an increase of 18% in the temperature range explored, the PL selectivity was the most sensitive to temperature variations.

TOF values were also calculated for the DHA conversion over FAU-AT2Ga in the various solvents at different temperatures. In view of the reported correlation between EL selectivity and

Table 2. Turnover frequency, conversion of dihydroxyacetone, and selectivity to alkyl lactates over FAU-AT2Ga as a function of the temperature (in C_1-C_4 alcoholic media).

Solvent	*T* (K)	*TOF*[a] (mol_{AL} mol_{LAS}^{-1} h^{-1})	X_{DHA} (%)	S_{AL} (%)
methanol	363	92	99	73
	378	138	99	75
	393	164	99	82
ethanol	363	62	99	82
	378	75	99	91
	393	135	99	91
n-propanol	363	52	99	73
	378	62	99	84
	393	89	99	91
n-butanol	363	45	99	75
	378	51	99	85
	393	84	99	88

[a] calculated as mole of AL formed per mole of Lewis-acid sites (LAS) per unit time during the first 0.5 h.

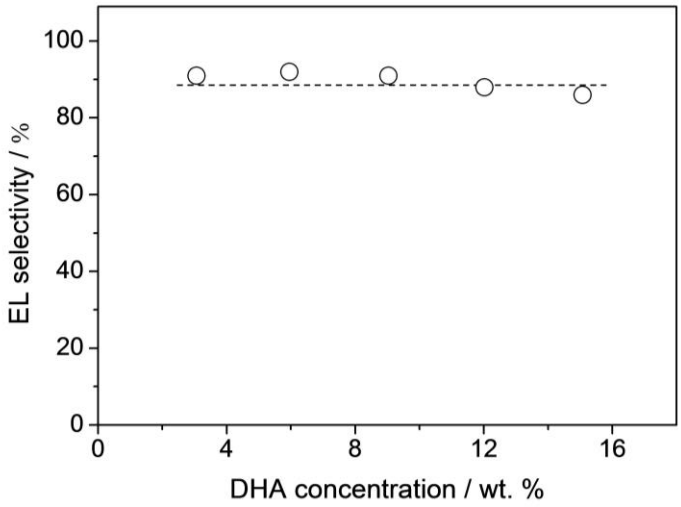

Fig. 7. EL selectivity *versus* DHA feed concentration over FAU-AT2Ga at 393 K.

amount of Lewis-acid sites of the zeolites [22], the TOF was most appropriately calculated based on the concentration of Lewis-acid sites in the catalyst. The initial reaction rates increased at higher temperatures and at decreasing size of the alcohol molecules (Table 2). In fact, the highest value was reached for ML at 393 K, while the lowest was observed for BL at 363 K.

Finally, as studies on the chemo-catalytic conversion of DHA have usually been undertaken in diluted feeds (3 wt.% in the substrate), the possibility to employ higher feed concentrations has been explored. This assessment represents a logical extension after having demonstrated the stability of FAU-AT2Ga in consecutive catalytic cycles in ethanol [22]. Accordingly, FAU-AT2Ga was tested in ethanol at 393 K at DHA feed concentrations up to 15.0 wt.%, while keeping the amount of catalyst constant. Its outstanding activity and selectivity were preserved under all conditions (Fig. 7). The possibility of increasing the process productivity is highly relevant in the perspective of a large-scale application of this system.

4. Conclusions

Post-synthetic modification of FAU-type zeolite was studied for the liquid-phase isomerization of bio-based dihydroxyacetone to alkyl lactates. Alkaline treatment in the presence of a gallium salt was demonstrated to generate more selective catalysts for the production of ethyl lactate compared to conventional methods for metal incorporation such as dry impregnation and ion exchange. This is attributed to the creation of larger amounts of highly selective tetra-coordinated Lewis-acid centers. Alkaline-assisted galliation was also successfully applied to a variety of other zeolite frameworks including FER, MOR, MFI, and BEA, although the performance of galliated FAU was unrivalled. The latter catalyst also proved highly efficient in the isomerization of DHA in various short-chain alcohols, achieving full conversion and the highest selectivities reported so far for any tin-free catalyst for the production of *n*-propyl and *n*-butyl lactates, besides ethyl lactate, under mild conditions. Higher temperatures were beneficial for the selectivity of the process and enhanced the production rates of the shorter alcohols, especially. The remarkable performance of galliated FAU in ethanol could be retained upon increasing up to five times the initial feed concentration of dihydroxyacetone. Overall, versatility and robustness add up to the outstanding Lewis-acid properties of FAU modified by galliation in basic media making it an attractive catalyst for the industrial production of bio-derived alkyl lactates.

Acknowledgements

This work was supported by the Swiss National Science Foundation (Project Number 200021-140496). Dr. R. Verel and Dr. S. Mitchell are gratefully acknowledged for MAS NMR spectroscopy and TEM analyses, respectively. Mr. M. J. Menart is thanked for experimental input.

References

[1] A. Corma, S. Iborra, A. Velty, Chem. Rev. 107 (2007) 2411-2502.

[2] S. Van de Vyver, Y. Román-Leshkov, Catal. Sci. Technol. 3 (2013) 1465-1479.

[3] P. Mäki-Arvela, T. Salmi, B. Holmbom, S. Willför, D. Yu. Murzin, Chem. Rev. 111 (2011) 5638-5666.

[4] T. Ståhlberg, W. Fu, J. M. Woodley, A. Riisager, ChemSusChem 4 (2011) 451-458.

[5] C. L. Williams, C. -C. Chang, P. Do, N. Nikbin, S. Caratzoulas, D. G. Vlachos, R. F. Lobo, W. Fan, P. J. Dauenhauer, ACS Catal. 2 (2012) 935-939.

[6] P. Y. Dapsens, C. Mondelli, J. Pérez-Ramírez, ACS Catal. 2 (2012) 1487-1499.

[7] M. Dusselier, P. Van Wouwe, A. Dewaele, E. Makshina, B. F. Sels, Energy Environ. Sci. 6 (2013) 1415-1442.

[8] S. P. Chahal and J. N. Starr, in Ullmann's Encyclopedia of Industrial Chemistry, Wiley-VCH Verlag, 2006, pp. 219-226.

[9] C. S. M. Pereira, V. M. T. M. Silva, A. E. Rodrigues, Green Chem. 13 (2011) 2658-2671.

[10] Y. Hayashi, Y. Sasaki, Chem. Commun. (2005) 2716-2718.

[11] E. Taarning, S. Saravanamurugan, M. S. Holm, J. Xiong, R. M. West, C. H. Christensen, ChemSusChem 2 (2009) 625-627.

[12] M. S. Holm, S. Saravanamurugan, E. Taarning, Science 328 (2010) 602-605.

[13] R. M. Painter, D. M. Pearson, R. M. Waymouth, Angew. Chem., Int. Ed. 49 (2010) 9456-9459.

[14] R. S. Assary, L.A. Curtiss, J. Phys. Chem. A 115 (2011) 8754-8760.

[15] P. P. Pescarmona, K. P. F. Janssen, C. Delaet, C. Stroobants, K. Houthoofd, A. Philippaerts, C. De Jonghe, J. S. Paul, P. A. Jacobs, B. F. Sels, Green Chem. 12 (2010) 1083-1089.

[16] R. M. West, M. S. Holm, S. Saravanamurugan, J. Xiong, Z. Beversdorf, E. Taarning, C. H. Christensen, J. Catal. 269 (2010) 122-130.

[17] Q. Guo, F. Fan, E. A. Pidko, W. N. P. van der Graaff, Z. Feng, C. Li, E. J. M. Hensen, ChemSusChem 6 (2013) 1352-1356.

[18] J. Wang, Y. Masui, M. Onaka, Appl. Catal., B 107 (2011) 135-139.

[19] L. Li, C. Stroobants, K. Lin, P. A. Jacobs, B. F. Sels, P. P. Pescarmona, Green Chem. 13 (2011) 1175-1181.

[20] C. Hammond, S. Conrad, I. Hermans, Angew. Chem., Int. Ed. 51 (2012) 11736-11739.

[21] P. Y. Dapsens, C. Mondelli, J. Pérez-Ramírez, ChemSusChem 6 (2013) 831-839.

[22] P. Y. Dapsens, M. J. Menart, C. Mondelli, J. Pérez-Ramírez, Green Chem. (2013) DOI: 10.1039/C3GC40766G.

[23] K. Lin, L. Li, B. F. Sels, P. A. Jacobs, P. P. Pescarmona, Catal. Today 173 (2011) 89-94.

[24] J. Pérez-Ramírez, S. Mitchell, D. Verboekend, M. Milina, N. -L. Michels, F. Krumeich, N. Marti, M. Erdmann, ChemCatChem 3 (2011) 1731-1734.

[25] G. Giannetto, G. Leon, J. Papa, R. Monque, R. Galiasso, Z. Gabelica, Catal. Today 31 (1996) 317-326.

[26] C. Otero Arean, A. Lopez Bellan, M. Penarroya Mentruit, M. Rodriguez Delgado, G. Turnes Palomino, Microporous Mesoporous Mater. 40 (2000) 35-42.

[27] H. K. C. Timken, E. Oldfield, J. Am. Chem. Soc. 109 (1987) 7669-7673.

[28] T. Takeguchi, K. Kagawa, J. B. Kim, T. Inui, D. Wei, G. L. Haller, Catal. Lett. 46 (1997) 5-9.

[29] D. Verboekend, J. Pérez-Ramírez, Catal. Sci. Technol. 1 (2011) 879-890.

[30] A. N. C. van Laak, R. W. Gosselink, S. L. Sagala, J. D. Meeldijk, P. E. de Jongh, K. P. de Jong, Appl. Catal., A 382 (2010) 65-72.

Electronic Supplementary Information

Gallium-modified zeolites for the selective conversion of bio-based dihydroxyacetone into C_1-C_4 alkyl lactates

Pierre Y. Dapsens, Bright T. Kusema, Cecilia Mondelli*, Javier Pérez-Ramírez*

ETH Zurich, Institute for Chemical and Bioengineering, Department of Chemistry and Applied Biosciences, Wolfgang-Pauli-Strasse 10, CH-8093 Zurich, Switzerland

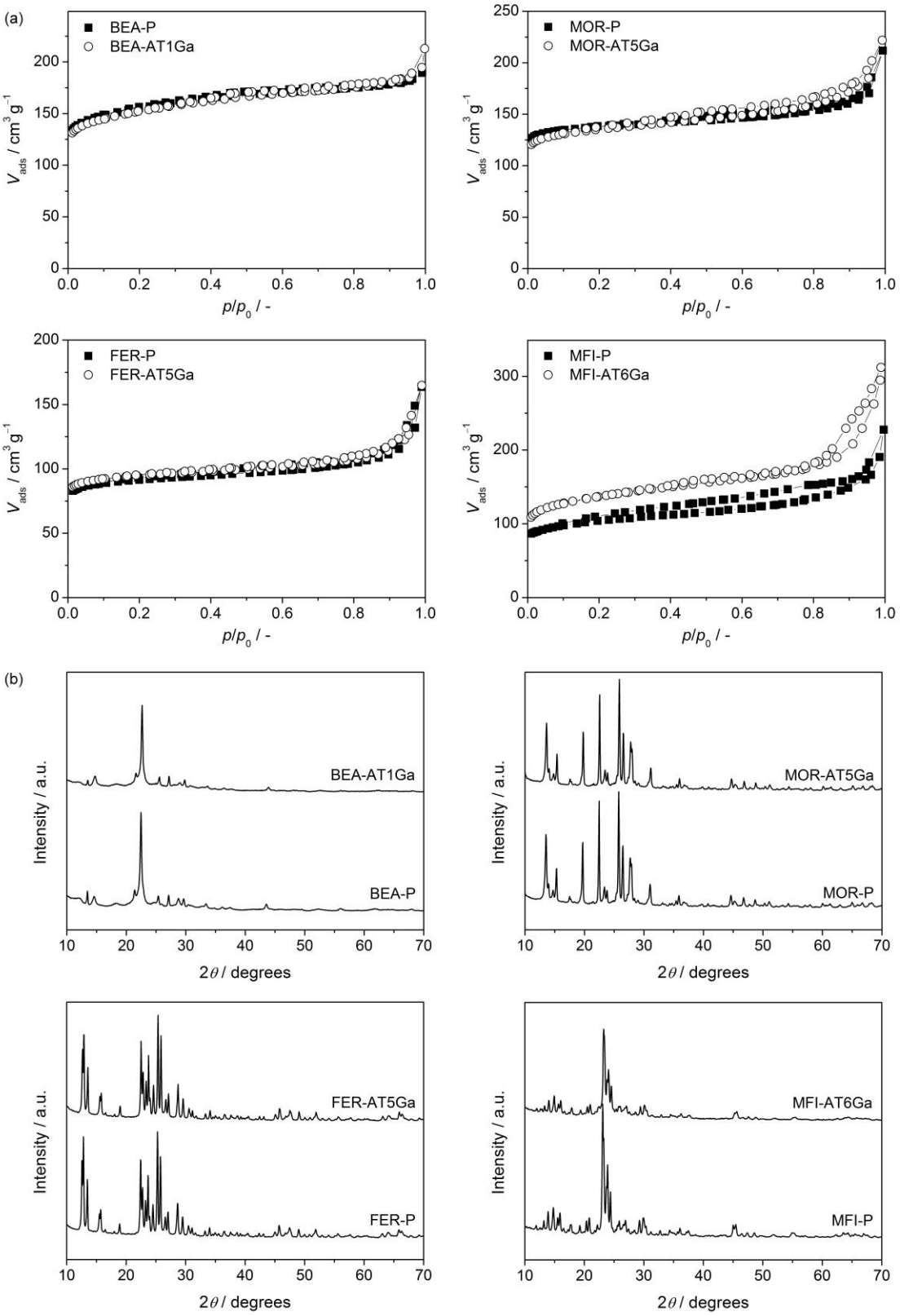

Fig. SI1. (a) N_2 isotherms and (b) X-ray diffraction patterns of BEA, MOR, FER, and MFI zeolites in parent form and after alkaline-assisted galliation.